AL45 - Thermal Conductivity Measurement and Heat Loss Analysis of Anode Cover Material for Aluminium Reduction Cell

Tao Yang[1], Jun Huang[2], Aihua Gao[3], Ye Qiu[4] and Shiping Yu[5]
1. Department deputy general manager
2. Professorate senior engineer
3. Business executive
4. Business assistant
5. Translator
CHALIECO GAMI, Guiyang, Guizhou, China
Corresponding author: ytdazei@126.com

Abstract

In an aluminium reduction cell, more than half of the heat loss is dissipated through the anode and the top cover. The thermal resistance of the anode cover is a key component. This paper proposes to measure thermal conductivity of the cover material using plate thermal conductivity meter to guide the design and operation of the aluminium reduction cell. The authors sample and test the thermal conductivity of the crushed cover material and fresh alumina powder on the anode, and compare the thermal conductivity of the cover materials with different particle sizes, and analyze the temperature and heat dissipation of different anode cycles. At the end, some suggestions are made on the selection of the particle size, composition ratio and thickness of anode cover material in the aluminium reduction cell operation, and a new method of anode covering is proposed.

Keywords: Aluminium reduction cell, Anode top heat loss, Anode cover material, Thermal resistance.

1. Introduction

Thermal equilibrium of an aluminium reduction cell is mainly related to the temperature field distribution of each part of the cell. The temperature field has a direct influence on the service life of the cell: over-insulation will cause poor cell ledge and lead to side corrosion and early failure while weak insulation may result in a thick cell ledge and put too much pressure on the cell. During cell operation, a 120–200 mm cover mainly composed of crushed bath and alumina, should be laid on the anode. This work can be done manually or by crane. The anode cover has three main functions: to adjust and control the cell thermal equilibrium, prevent anode oxidation and serve as the first barrier against hydrogen fluoride emission.

However, there are some problems in the anode cover management during operation, such as: too long time for anode changing which makes it hard to achieve standardized control; the laying of cover material is completely controlled by workers and the thickness of the cover material is uneven, resulting in poor thermal insulation uniformity; the replacement of butt will generate heat loss, and the new anode cover will absorb heat too when it enters the operation process.

Therefore, a better understanding of anode cover characteristics and a standardized anode cover method would help to improve heat dissipation distribution and maintain a good thermal equilibrium condition for cells. Smelters have different methods for anode cover; some lay cover material on the new anode before anode change, and then move the new anode and its cover to the cell simultaneously; others replace the anode first and lay cover material a few hours later.

In this experiment we took samples of cover material and alumina from two smelters and compared the thermal conductivity of cover materials with different particle sizes. In this paper, the authors intend to analyze anode cover from the perspective of heat dissipation of cell, optimize the ratio and the laying method of the cover material through a thermal conductivity test. The goal is to seek a better operational solution to maintain the energy balance of the aluminium reduction cell.

2. Analysis on Heat Loss from Cell Upper Structure

The heat loss from the upper part of the cell accounts for more than 50 % of the total heat loss. The thickness of the thermal insulation material has a decisive influence on the heat loss of the upper cell. Therefore, a stable and uniform heat insulation layer is crucial to maintaining the energy balance of the cell. At present, a common problem for Chinese prebaked cells is an insufficient heat insulation material. Obviously, the thinner the heat insulation material is, the higher the ratio of heat loss from the top of the cell to the total heat loss, and changes in the material surface are more likely to cause changes in the energy balance (or thermal equilibrium), so the stability of cell gets worse. The typical heat loss of modern aluminium reduction cells is roughly as follows: more than 50 % of the heat is dissipated from gas, hood and upper structure after passing through the anode cover material, and around 40 % is dissipated from the side and end of the cell, and only less than 10 % is dissipated from the bottom of the cell [1].

The heat loss of the cell can be divided into two regions, as shown in Figure 1 below.

Region A: due to the crust and leg on the side of the cell, the temperature at the interface between the crust and the cell is constrained by the initial crystal temperature of the bath. Therefore, the heat loss from the cell shell relates to the heat loss of the bath superheat (T_{bath}-T_{liq}).

Region B: it is related to the heat loss transmitted under bath temperature condition.

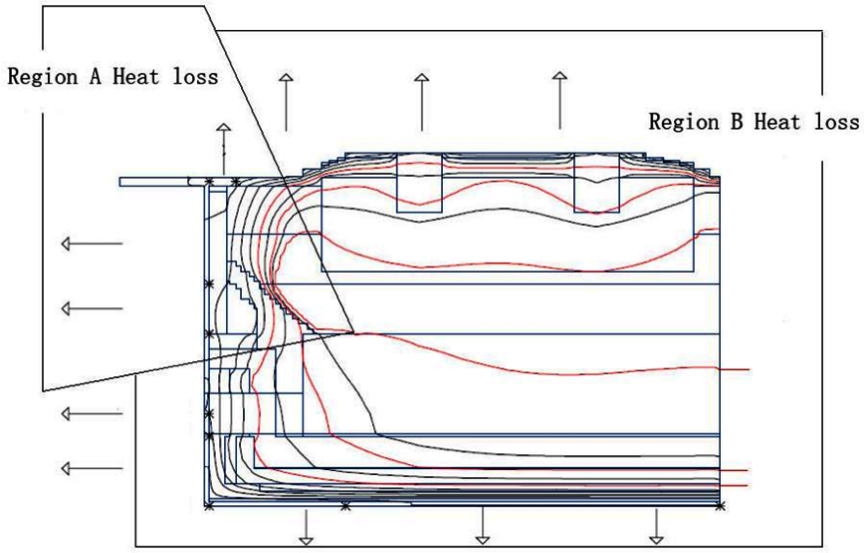

Figure 1. Two regions of heat loss in the aluminium reduction cell.

The thermal resistance of the upper part of the cell mainly consists of three parts: the convection heat transfer resistance of bath and anode, the thermal conductivity resistance of the anode and cover material, and the convection heat transfer resistance of the cover material and gas. The total thermal resistance of the upper cell is shown in the following equation:

$$R = \frac{1}{\alpha_1} + \frac{\delta_1}{\lambda_1} + \frac{\delta_2}{\lambda_2} + \frac{1}{\alpha_2} \quad (1)$$

where:

α_1, α_2 Convection heat transfer coefficients of the bath and anode, of the cover material and gas, respectively, W/(m^2·K)

δ_1, δ_2 Height of the anode and cover material, m

λ_1, λ_2 Thermal conductivity of the anode and cover material, W/(m·K)

Compare the weights of various thermal resistances. Firstly, according to references, the convection heat transfer coefficient of bath and anode mostly ranges from 600 to 1200 W/(m^2·K), with a thermal resistance range of 0.00083 to 0.0017 (m^2·K)/W; the average height of the anode is calculated as 350 mm, and its thermal conductivity is taken as 5.5 W/(m^2·K), then the thermal resistance of the anode is 0.064 (m^2·K)/W; the average height of the cover layer is calculated as 180 mm, and its thermal conductivity value is 0.5 W/(m^2·K), resulting in a thermal resistance of 0.36 (m^2·K)/W. The convection and radiation heat transfer coefficient of the cover material layer and the gas ranges from 15 to 22 W/(m^2·K), and its thermal resistance range is 0.045 to 0.067 (m^2·K)/W. By comparing these various thermal resistances, it can be seen that the thermal resistance of the cover material accounts for approximately 70 % of the total thermal resistance of the top of the cell.

3. Thermal Conductivity Measurement

For thermal conductivity measurement we use a plate thermal conductivity meter. Based on the basic principle of Fourier's one-dimensional flat plate stable thermal conductivity process, after the one-dimensional heat flow longitudinally passes through the hot surface of the sample to the cold surface of the sample during steady state, the heat carried away by the water in the calorimeter is measured. The heat Q is directly proportional to the thermal conductivity, and inversely proportional to the temperature difference T_2-T_1 between the hot and cold surfaces of the sample. The instrument calculates the thermal conductivity λ by measuring Q and (T_2-T_1) [2-3]

$$\lambda = \frac{dQ}{A(T_2 - T_1)} \quad (2)$$

where：

λ Thermal conductivity of material, W/(m·K)

T_2 Setting temperature of hot surface, ℃

T_1 Setting temperature of cold surface, ℃

A Surface area of central heating plate, m^2

Q Heat transfer power of central heating plate, W

d Thickness of test piece, m

3.1 Cover Particles Removed from New Anode

Random samples of the covers were taken from a new anode of a 200 kA aluminium reduction cell for measurements. The samples were divided into two groups, one with bigger particle size and another with smaller particle size. Then the samples were heated during the measurements. When the temperature reached 200 ℃, thermal conductivity measurements were made every 50 ℃ increase in temperature up to 800 ℃.

The measurement results are: the thermal conductivity of sample 1 is 0.334 W/(m·K) when the temperature reaches 200 ℃; as the temperature rises, its thermal conductivity increases to a maximum of 0.481 W/(m·K) at 600 ℃ and gradually decreases to 0.462 W/(m·K) at 800 ℃. The thermal conductivity of sample 2 is 0.243 W/(m·K) at 200 ℃, and increases to 0.460 W/(m·K) at 800 ℃. The results for both samples are shown in Figure 2.

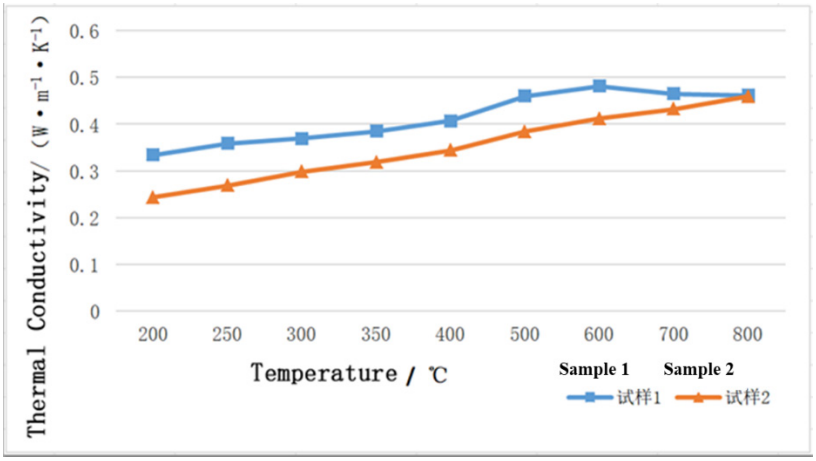

Figure 2. Thermal conductivity of cover layer increases with temperature.

3.2 Covers Removed from a Butt

The solid cover, which was removed from an anode butt of a 200 kA cell (Figure 3), is too hard to be measured, so it was grinded before measuring.

Figure 3. Solid cover removed from the butt of 200 kA cell.

The measuring result shows that the thermal conductivity of the grounded sample is 0.353 W/(m·K) at 300 ℃, and increases to 0.413 W/(m·K) at 800 ℃ (Figure 4).

The solid cover removed from an anode butt of 230 kA cell (Figure 5) was also grinded before measuring. The measurement shows that the thermal conductivity of the sample is 0.26 W/(m·K) at 200 ℃, and increases to 0.575 W/(m·K) at 800 ℃ (Figure 6).

After screening, the distribution range of particle size was: the weight proportion of materials with particle size greater than 10 mesh (< 2 mm) was 62.7 %, the weight proportion of materials

with particle sizes between 5 and 10 mesh (2-4 mm) was 37.3 %, and the weight proportion of materials with particle sizes less than 5 mesh (> 4 mm) was 0. It is important to specify particle size distribution since it has been shown that the thermal conductivity depends no particle size [4].

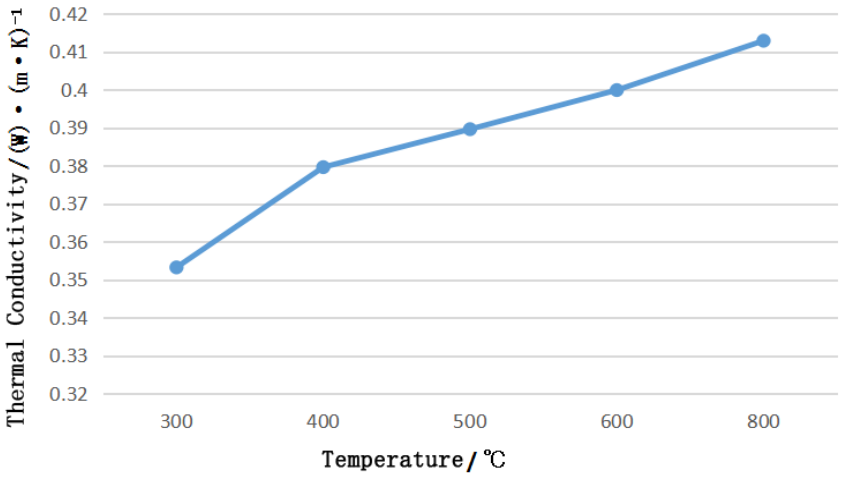

Figure 4. Thermal conductivity of grinded solid cover from an anode butt of a 200 kA cell increases with temperature.

Figure 5. Solid covers removed from an anode butt of a 230 kA cell.

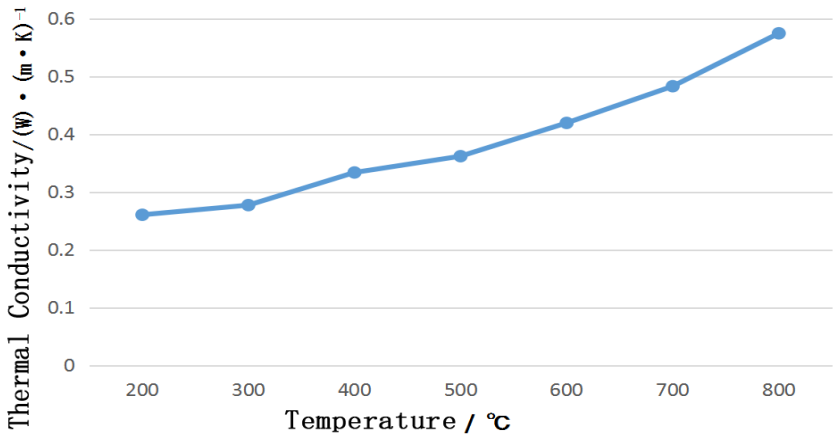

Figure 6. Thermal conductivity of grinded solid cover from an anode butt of a 230 kA cell increases with temperature.

3.3 Fresh Alumina Powder

Figure 7 shows the selected pure fresh alumina powder for measurement.

Figure 7. Alumina sample placed in heat conductor.

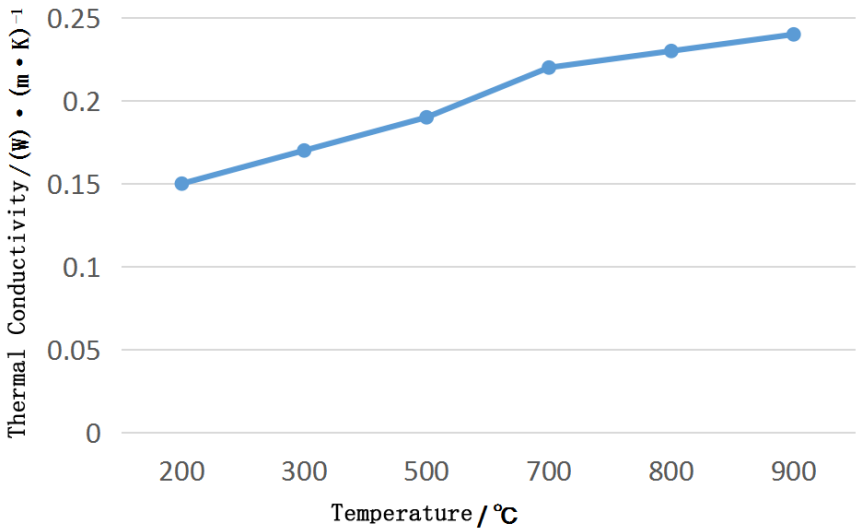

Figure 8. Thermal conductivity of alumina increases with temperature.

The measurement result shows that the thermal conductivity of the sample is 0.15 W/(m·K) at 200 °C, and increases to 0.24 W/(m·K) at 900 °C.

From the results, it can be seen that the thermal conductivity of the cover layer ranges from 0.2 to 0.6 W/(m·K), and the thermal conductivity of alumina powder ranges from 0.15 to 0.25 W/(m·K), both of which increase as the temperature increases. Based on the color of the samples after testing, it can be seen that the composition of the cover of the cell is relatively

complex. After high-temperature measurement and cooling of the samples, blue and pink particles appeared.

Our results agree with the data in literature for thermal conductivity of crushed bath [5], shown in Figure 6. We can see that in these data, thermal conductivity also increases with temperature.

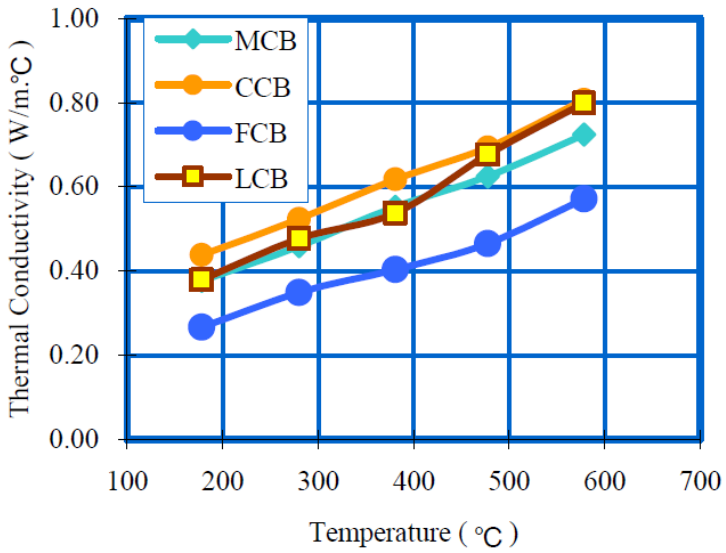

	LCB	FCB	MCB	CCB
Void Fraction	0.478	0.447	0.377	0.348

Figure 9. Thermal conductivity of crushed bath from [5] for different void fractions quoted below the graph. LCB – no sub 1mm fraction, FCB – no plus 150 µm fraction, MCB – between 150 µm and 1mm, CCB – combined material.

4. Temperature Measurement of Anode Covers

Temperature of the anode covers of aluminium reduction cells is measured in this experiment. The corresponding cover layers of different anode operating cycles were selected for measuring, with one set of high (newer) anode, one set of medium height anode (the anode that has run nearly half of the anode change cycle), and one set of low anode (the anode that is about to become a butt). Each group of selected anodes has three measuring points, as shown in Figure 10. Test point A is located towards the side of the cell, test point B is located in the middle of the anode, and test point C is located close to the center of the cell.

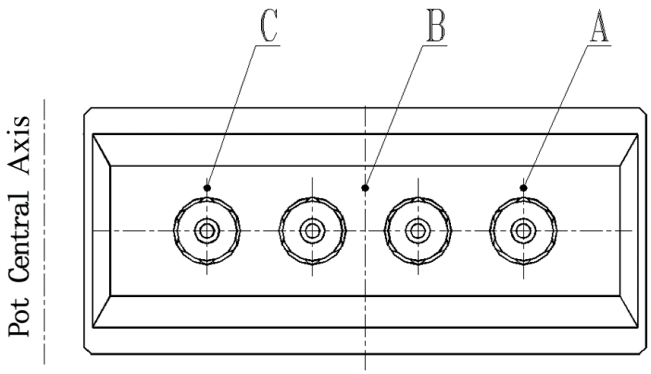

Figure 10. Temperature measuring points for the anode cover.

Tables 1 and 2 are measured data for 230 kA cell anode cover.

Table 1. Anode cover surface temperature test 1.

Height of cover/mm	Temperature (point A)	Temperature (point B)	Temperature (point C)
180 (high anode)	128	151	196
180 (medium height anode)	275	268	328
150~160 (low anode)	266	310	363

Table 2. Anode cover surface temperature test 2.

Height of cover/mm	Temperature (point A)	Temperature (point B)	Temperature (point C)
180 (high anode)	153	153	207
180 (medium height anode)	263	326	364
150~160 (low anode)	347	425	486

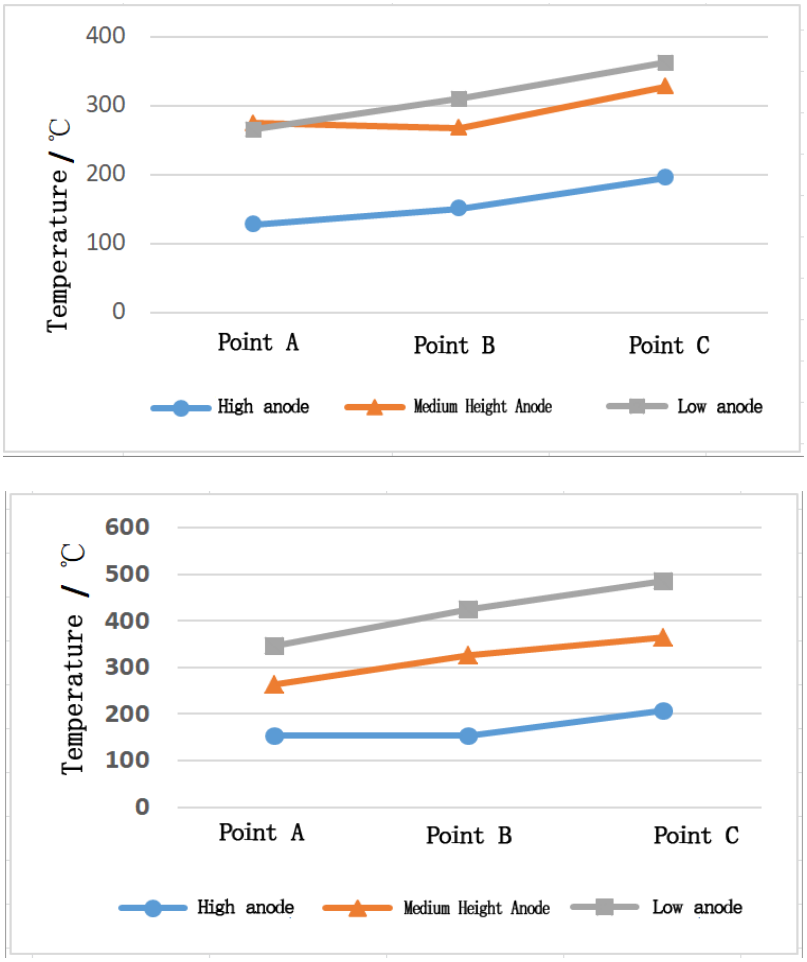

Figure 11. Anode cover surface temperature test 1 (top) and 2 (bottom).

From the measuring results it can be seen that after anode change, the surface temperature of the anode cover is relatively low when the anode is barely consumed, and it increases when the anode gradually consumes. During this process, the temperature increases by 20 to 50 %, with temperature increase of about 50–140 °C.

In addition, Table 1 shows the measured data of anode cover with different heights. When anode cover height drops from 180 mm to 150–160 mm, the temperature change is twice as big as before with the same anode consumption (i.e., same anode height) with an absolute temperature difference between 140 and 280 °C.

From the comparison of these two aspects - the surface temperature measurements of different anode heights and of different anode covers - it can also be seen that the change in anode cover height has a greater impact on the temperature of the anode cover surface.

5. Conclusions

In the current aluminium reduction operation, the anode cover layer has a significant impact on the thermal equilibrium and energy balance of the cell. The composition of the anode cover layer is a mixture of bath and alumina particles of different sizes. Due to the lower thermal conductivity of alumina compared to bath particles, to reduce the heat loss of the cell, the ratio of alumina in the cover layer can be increased. Also, the thickness of the cover layer can be increased.

The cover is mainly added manually or by crane. However, it is difficult for smelters to maintain standardization of anode cover for a long time. Therefore, the next step is to develop a reusable anode cover and related device. A new anode cover method and device would be beneficial for smelter construction, as it can reduce the construction investment and operating costs of crushing, conveying and feeding systems. Also, it would be helpful for smelter management, as it can reduce the workload and time required to maintain the operations (breaking, laying, and edge trimming) for existing anode cover work.

6. References

1. Yexiang Liu and Jie Li, *Modern Aluminum Electrolysis* [M], Beijing, Metallurgical Industry Press, 2008, 361-362.
2. Yajing Zhang, Qiang Zheng, Xigao Liu, et al., Thermal Conductivity Test of Refractory Materials, (Refractory materials. Determination of thermal conductivity (calorimeter)), *YB/T 4130-2005* [S], 2005, 1-5, https://www.chinesestandard.net/Related.aspx/YBT4130-2005.
3. Yunfeng Zhou, Changlin Li, Dengpeng Chai, et al., Study on properties of aluminium electrolytic anode cover material, *Chinese Light Metals*, 2015 (09), 32-35.
4. Changlin Li et al., Influence of cover material particle size composition on its physical property and insulation performance, *Light Metals* 2020, 653-658.
5. Mark P Taylor, Anode cover material – science, practice and future needs, *Ninth Australasian Aluminium Smelting Technology Conference and Workshops*, Terrigal, Australia, 4 – 9 November 2007, Paper 11.